Porphyrin Clathrates. Crystal Structures of Two Unexpected Products Obtained by Solvothermal Reactions of Pt-tetra(4-carboxyphenyl)porphyrin with Copper Acetate

MICHAELA SHMILOVITS, MIKKI VINODU and ISRAEL GOLDBERG*
School of Chemistry, Sackler Faculty of Exact Sciences, Tel Aviv University, 69978 Ramat Aviv, Tel Aviv, Israel

Abstract

Reactions between platinum tetra(4-carboxyphenyl)porphyrin and copper acetate in the presence of pyridine and either triethylamine or ammonium hydroxide, under solvothermal conditions, yielded 1:2 and 1:1 discrete porphyrin complexes with solvated copper ions. The latter crystallized from the respective reaction mixtures as channel-type lattice clathrates, accommodating pyridine or triethylamine in the interporphyrin channel voids. The host lattice consists of the Cu-coordinated porphyrin entities which stack one on top of the other in an offset manner at regular intervals of 3.8-4.1 Å. Side-packing of these stacks is stabilized by hydrogen-bonding interactions.

Introduction

Tetraarylporphyrins exhibit a high propensity to form clathrates due to the non-complementarity of their molecular shape in three-dimensional space [1, 2]. This feature, along with their unique chemical reactivity, makes them extremely useful in the design of new solid receptors. In this context, we have introduced earlier the *meso*-tetra(4-carboxyphenyl)porphyrin (TCPP) as a uniquely versatile building block for the construction of molecular sieve-type architectures, which may bear structural as well as functional resemblance to the inorganic zeolites [3–5]. The peripheral COOH-functional groups provide multiple attractive sites for cooperative intermolecular hydrogen bonding and for effective inter-coordination through external metal ion bridges in different directions. The latter is generally associated with deprotonation of the TCPP molecules during the reaction to account for charge balance, and formation of extended coordination polymers of "porous" crystalline architecture [5–8]. The dimensionality of these polymeric networks is affected to a large extent by the composition (whether single metal ions or metal ion clusters) and preferred coordination geometries of the bridging auxiliaries. Insertion of additional metal ions into the porphyrin core may serve to enhance the structural rigidity of the TCPP framework. The attractive zeolite sorption/desorption properties of such TCPP-based metalloporphyrin solids have been demonstrated in a most recent report [9].

As part of our continuing effort to formulate new 'porous' materials of this type [10, 11], we reacted in a basic environment (either ammonium hydroxide or triethylamine) the Pt-TCPP building blocks with copper acetate, Cu(OAc)$_2$, under solvothermal conditions. Platinum(II) cations reveal preference for square-planar coordination environment, and are thus perfect candidates for stabilizing a flat conformation of the porphyrin macrocycle free of axial ligands. The copper acetate is a readily available source for metal ions which can act as effective linkers between the carboxyporphyrin building blocks. Moreover, facile replacement of the acetate ligands by the carboxylate functions of the porphyrin is seemingly feasible. To our knowledge, structural determinations of coordination complexes based on these two components have not been reported prior to our work on this system. In previous studies, the reaction of external metal ion auxiliaries with TCPP building blocks yielded open network coordination polymers composed of the porphyrin units inter-coordinated through their four carboxylic arms by the metal ions, each of these ions (or ion clusters) being linked in turn to several porphyrin moieties. However, in this study unexpected products have emerged as well. They involve discrete coordination complexes **1** and **2**, wherein the copper metal ions are coordinated to a single porphyrin moiety, which crystallize as lattice clathrates. The synthesis and composition of **1** and **2**, as characterized precisely by X-ray diffraction, is shown in Scheme 1 below.

---

* Author for correspondence. E-mail: goldberg@post.tau.ac.il
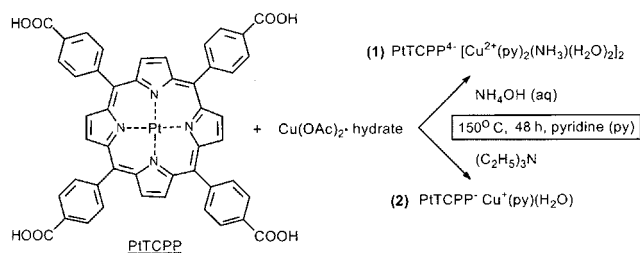
Scheme 1. The syntheses of complexes **1** and **2**. The PtTCPP^{4-} and PtTCPP^{-} anions represent the tetra- and mono-deprotonated porphyrin species, respectively.

Experimental section

General

The platinum tetra(4-carboxyphenyl)porphyrin was procured commercially from Porphyrin Systems GbR. Other reagents and solvents were obtained from J.T. Baker (pyridine), Merck (triethylamine), Aldrich (copper bi-acetate hydrate) and Frutarom (ammonium hydroxide). All the starting materials were used without further purification.
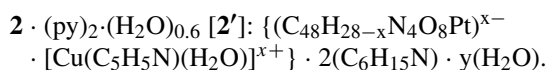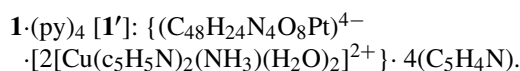
Preparative procedures

The complexes were synthesized under solvothermal conditions, placing a mixture of the reactants and solvents in a small sealed reactor, continuously heating the reaction mixture at about 150 °C for four days, and then gradually cooling the resulting products over the period of 24 h to ambient room temperature. The reacting components included about 5 mg (0.0056/0.0051 mmol) of the porphyrin, 4.75 mg (0.0026 mmol) of Cu(OAc)$_2$ hydrate, 0.5 ml of triethylamine or ammonium hydroxide as the base reagent to assist in de-protonation of the carboxylic functions, and 0.5–0.8 ml pyridine as porphyrin solubilizing agent. The yields of the crystalline clathrate products **1**·(py)$_4$ and **2**·(py)$_2$·(H$_2$O)$_{0.6}$ were generally on a 1-2 milligram scale in a single reaction run. The uniformity of the formed compounds was confirmed in each case by repeated measurements of the unit-cell dimensions from several randomly chosen single crystallites. The solvent content was assessed also independently by thermo-gravimetric measurements of weight loss upon heating samples of the corresponding materials.

Crystallography

The diffraction measurements were carried out on a Nonius KappaCCD diffractometer, using graphite monochromated MoKα radiation (λ = 0.7107 Å). The crystalline samples of the analyzed compounds were covered with a thin layer of light oil and freeze-cooled to *ca*. 110 K in order to minimize solvent escape, structural disorder and thermal motion effects, and increase the precision of the results. The structures were solved by direct methods (SIR-97 [12]), and refined by full-matrix least-squares on F^2 (SHELXL-97 [13]). Intensity data were corrected for absorption effects. All non-hydrogen atoms (except of those of the severely

disordered solvents) were refined anisotropically. The hydrogens were either found in difference-Fourier maps or located in idealized positions, and were refined using a riding model with fixed thermal parameters [$U_{ij} = 1.2U_{ij}$ (eq.) for the atom to which they are bonded]. No phase transitions of the two crystalline compounds were detected between room temperature and 110 K. The structural formulae of the two crystalline compounds are:

1·(py)$_4$ [**1'**]: {(C$_{48}$H$_{24}$N$_4$O$_8$Pt)$^{4-}$
·[2[Cu(c$_5$H$_5$N)$_2$(NH$_3$)(H$_2$O)$_2$]$^{2+}$}· 4(C$_5$H$_4$N).

2 · (py)$_2$·(H$_2$O)$_{0.6}$ [**2'**]: {(C$_{48}$H$_{28-x}$N$_4$O$_8$Pt)$^{x-}$
· [Cu(C$_5$H$_5$N)(H$_2$O)]$^{x+}$} · 2(C$_6$H$_{15}$N) · y(H$_2$O).

Optimal values for x = 0.65 and y = 0.55 were determined by best convergence of the crystallographic refinement against the diffraction data.

The crystal data of **1'** and **2'** are given in Table 1. Initially the crystallographic refinement of **2'** converged poorly at R = 0.08, and the atomic displacement parameters associated with atoms in the Cu(py)(H$_2$O) fragment were 2–3 times larger than within the porphyrin moiety. Acceptable parameters were obtained only when its occupancy factor was allowed to vary (being reduced from 1.0 to 0.65), and partial racemic twinning was assumed.

In **1'**, molecules of the complex are located on centers of inversion. The crystal structure contains severely disordered solvent molecules of pyridine, which are located within the interporphyrin channels. The water protons were located in difference-Fourier maps. All the remaining hydrogen atoms were placed in calculated positions. In **2'**, all the hydrogen atoms were placed in calculated positions, taking into account the hydrogen-bonding interactions, as indicated by the relevant O···N and O···O contacts (Table 2), and observed residual electron density therein. The assigned oxidation state of +1 for the copper ions in this structure, which accounts for a charge-balanced material, is consistent with the typical linear or T-shaped (when the more distant water species is considered as well) coordination geometry found around this ion [14], and with the number of carboxylic protons required to optimize the hydrogen-bonding scheme (see below). Reduction of Cu^{2+} to Cu^{+} in basic amine environments is a well-known phenomenon [14]. No other experimental evidence is available to confirm this assignment, which however has little effect on the observed clathrate properties of this material.

Results and discussion

The results of this study reveal two different discrete entities of Cu-porphyrin complexes, **1** and **2**, rather than the anticipated networks of extended coordination polymers successfully constructed with other metal ions (in polymeric materials the metal ion auxiliary is coordinated to the carboxylate functions of four different porphyrin units, and every porphyrin is coordinated to four different bridging metal ions) [6, 9]. This "failure" in the present case should be attributed to the use of excess of the pyridine solvent

Table 1. Crystal data and parameters of the structural analysis

Clathrate	**1′**	**2′**
Molecular weight	1845.81	1300.59
Crystal system	Monoclinic	Monoclinic
Space group	$C2/c$	$P2_1$[a]
A (Å)	47.8140(6)	7.9630(2)
B (Å)	6.3050(1)	24.5440(8)
C (Å)	24.0110(7)	14.9550(4)
β (°)	130.628(1)	101.454(2)
V (Å^3)	7781.7(2)	2864.6(1)
Z	4	2
μ(MoKα) (mm^{-1})	2.41	2.75
T (°K)	110	110
D_c (g cm^{-3})	1.576	1.508
$2\theta_{max}$ (°	55.7	56.4
No. unique reflections	9009	11607
No. reflcs. with $I > 2\sigma$	6419	9682
No. refined parameters	531	735
R1 ($I > 2\sigma$)	0.045	0.044
R1 (all data)	0.072	0.061
wR2 (all data)	0.110	0.107
$|\Delta\rho|_{max}$/e Å^{-3}	1.03	2.21

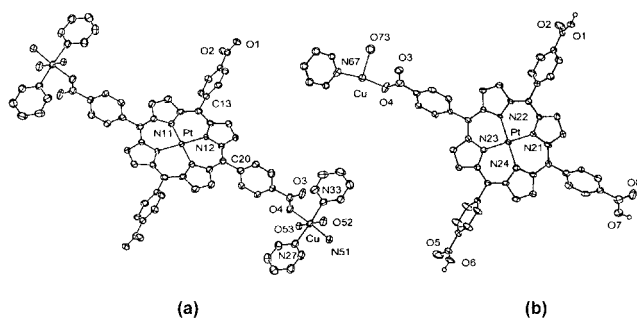[a] This structure refined as a 0.78:0.22 racemic twin.

Figure 1. Ortep view of the copper-coordinated complexes of the Pt-TCPP. The atom ellipsoids represent thermal displacement parameters at the 50% probability level at 110 K. (a) Complex **1**. Bond lengths involving the platinum ion in the porphyrin core are Pt—N11 2.020(4) and Pt—N12 2.021(4) Å. Those involving the copper moiety are: Cu—O4 1.952(3), Cu—N27 2.041(4), Cu—N33 2.049(4), Cu—N51 2.005(4), C···O52 2.374(4) and C···O53 2.513(4) Å. (b) Complex **2**. The corresponding bond distances are: Pt—N 2.001–2.028(4), Cu—O4 1.872(4), Cu—N67 1.936(7) and Cu—O73 2.360(6) Å. The Cu(py)(H$_2$O) residue has been refined with 65% occupancy, suggesting that it is coordinated to only two out of three Pt-TCPP units in the crystal. The solvent species accommodating interporphyrin voids in the two structures are not shown.

and presence of the ammonium hydroxide base in the reaction mixture. The pyridine and NH$_3$ (readily available from NH$_4$OH at high temperature) ligands are characterized by high coordinating affinity to copper ions, and by occupying some of the coordination sites prevent their multiple association with the porphyrin species. Thus, in the reaction products only two COO$^-$ groups in **1** and one COO$^-$ function in **2** were found to coordinate directly to Cu. The incomplete coordination observed in the latter case (see in Experimental Section) is most probably due to very low solubility of the copper acetate reagent in the respective reaction mixture (Scheme 1).
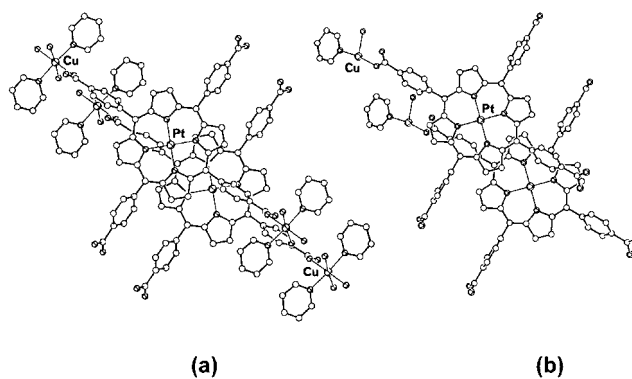

(a) **(b)**

Figure 2. Illustration of the parallel shift between the adjacent moieties within the porphyrins stacks in the crystals of: (a) **1′**, and (b) **2′**. All the non-C atoms are marked by crossed circles (H omitted).

The molecular structures of the two compounds are illustrated in Figure 1. The central core of the porphyrin moiety is nearly planar with only a slight roughening. The deviations of the individual atoms from the mean plane of the 24-atom macrocycle in the two structures are ≤ 0.08 Å. The platinum ion is four-coordinate, residing in the center of the porphyrin core. The carboxyphenyl rings are oriented roughly perpendicular to the porphyrin macrocycle, the corresponding twist angles being within 60–86°. The coordination bond lengths of the platinum ion to the pyrrole N-atoms, and of the external copper ion to the carboxylate O-atom, are given in Figure 1. The latter indicate strong Cu—CO$^-$ binding to the deprotonated hydroxylic O-atom. In **1**, the copper ion has a distorted octahedral environment, characteristic to d^9 Cu^{II}. It is strongly linked to the carboxylic function, two pyridine and one NH$_3$ ligands, and more weakly coordinated to two water molecules. One of the latter forms an intramolecular hydrogen bond to the carbonyl end of the proximate carboxylate (Table 2). The non-coordinated carboxylate groups are delocalized, the two C—O bond distances being nearly equal 1.261(6) and 1.270(6) Å, as opposed to the copper-coordinated functions wherein the corresponding bond lengths are distinctly different: C=O 1.235(6) and C—O(Cu) 1.289(6) Å. Correspondingly in **2**, the O-atoms of the longer carbon-oxygen bonds are either protonated or coordinated to the copper ion, though here the covalent parameters seem to be less consistent, as they represent average values of the carbon-oxygen bonds between the coordinated and the free Pt-TCPP units present in the crystal (the precision is also affected by the apparent crystal twinning). The corresponding carbon-oxygen bond length pairs are: C—OH(1) 1.282(7), C=O2 1.247(7), C=O3 1.259(6), C—O4(Cu) 1.307(7), C=O5 1.247(7), C—OH6 1.266(6), C—OH7 1.295(7) and C=O8 1.262(7) Å. In this structure, the copper ion is three-coordinate, the planar arrangement of the linked species being compatible with d^{10} Cu^I [14]. The molecular geometries of the constituent species are, otherwise, characterized by common features.

The emerging crystal structures of **1′** and **2′** represent channel-type clathrates with the copper-coordinated Pt-TCPP as host, and either pyridine in **1′**, or triethylamine in **2′**, as guests. They reveal characteristic features of the "por-
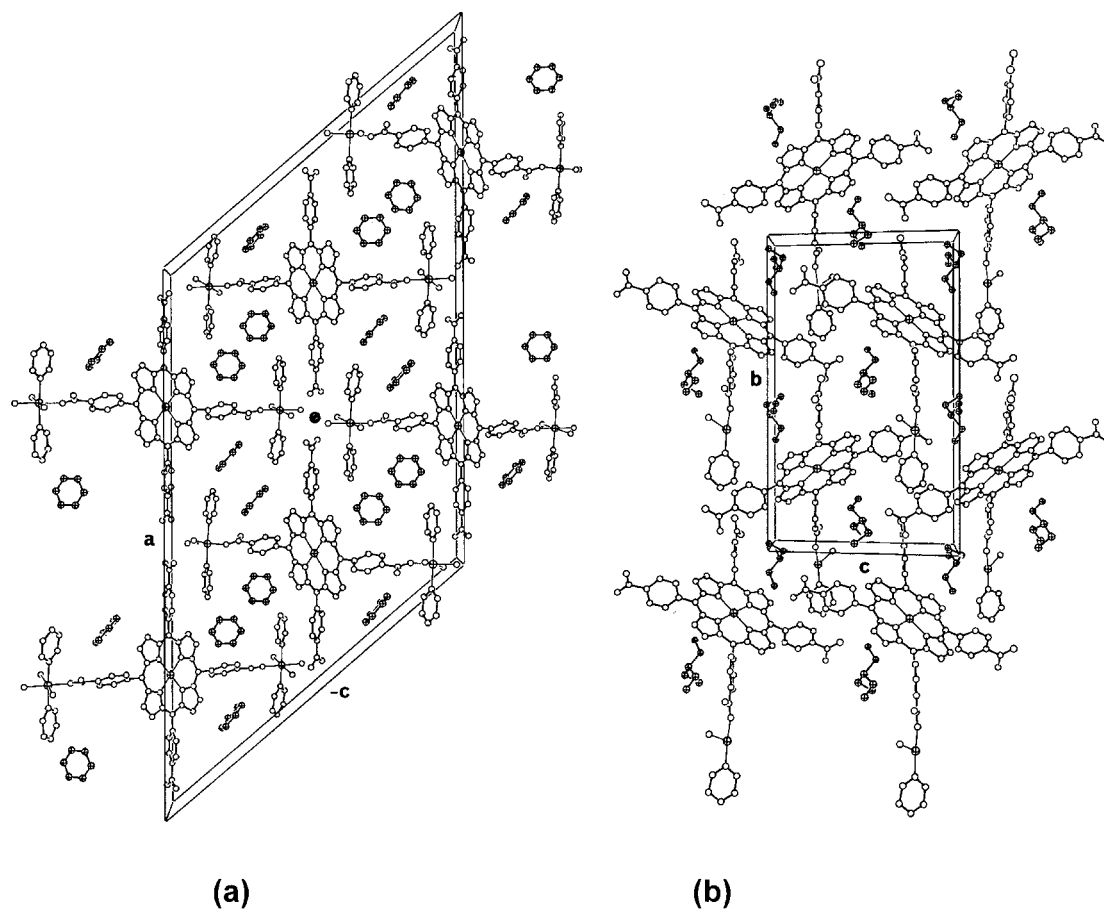
(a)   **(b)**

Figure 3. View of the crystal structures down the interporphyrin channel voids, which illustrates the stoichiometric enclathration of the guest components within the channels propagating through the crystal. (a) Structure **1′** viewed down the *b*-axis (*a* is vertical) of the crystal. There are no specific interactions between the porphyrin lattice and the pyridine solvent species. The black dot at $x = \frac{1}{2}$ and $z = \frac{1}{2}$ denotes the hydrogen-bonding site between four adjacent stacks (see Figure 4). (b) Structure **2′** viewed down the *a*-axis (water solvent omitted). The guest triethylamine molecules are hydrogen-bonded to the porphyrin columns (Table 2). The Pt and Cu atoms, as well as the guest components accommodating the interporphyrin channel voids are marked by crossed circles.

Table 2. Hydrogen-bonding parameters

D-H	A (N or O)	D-H (Å)	H-A (Å)	O···A (Å)	D-H···A (°)
Clathrate **1′**					
NH(51a)	O2 $(x, -y, z - \frac{1}{2})$	0.91	2.07	2.970(5)	169.2
NH(51b)	O1 $(x, 1 - y, z - \frac{1}{2})$	0.91	2.33	3.174(5)	153.4
NH(51c)	O1 $(-x, 1 + y, \frac{1}{2} - z)$	0.91	2.24	3.129(5)	165.8
OH(52b)	O3 (x, y, z)	0.92	1.77	2.674(5)	166.9
OH(52a)	O53 $(x, 1 + y, z)$	0.96	1.96	2.802(5)	144.6
OH(53a)	O2 $(-x, 1 + y, \frac{1}{2} - z)$	0.95	1.81	2.722(4)	161.6
OH(53b)	O1 $(x, -y, z - \frac{1}{2})$	0.96	1.81	2.728(4)	158.2
Clathrate **2′**					
OH(1)	N60 $(x + 1, y, z + 1)$	0.84	1.80	2.640(5)	174.7
OH(6)	N53 $(x - 1, y, z - 1)$	0.84	1.84	2.667(6)	169.7
OH(7)	O5 $(-2 - x, y + \frac{1}{2}, -z)$	0.84	1.72	2.542(6)	166.5
OH(73a)	O3 (x, y, z)	0.86	1.93	2.788(8)	180
OH(73b)	O1 $(2 - x, y - \frac{1}{2}, 1 - z)$	0.82	1.84	2.660(8)	180
OH(74a)	O6 $(x + 1, y, z + 1)$	0.88	2.01	2.893(9)	180
OH(74b)	O8 $(-x, y - \frac{1}{2}, 1 - z)$	0.88	2.02	2.908(9)	180

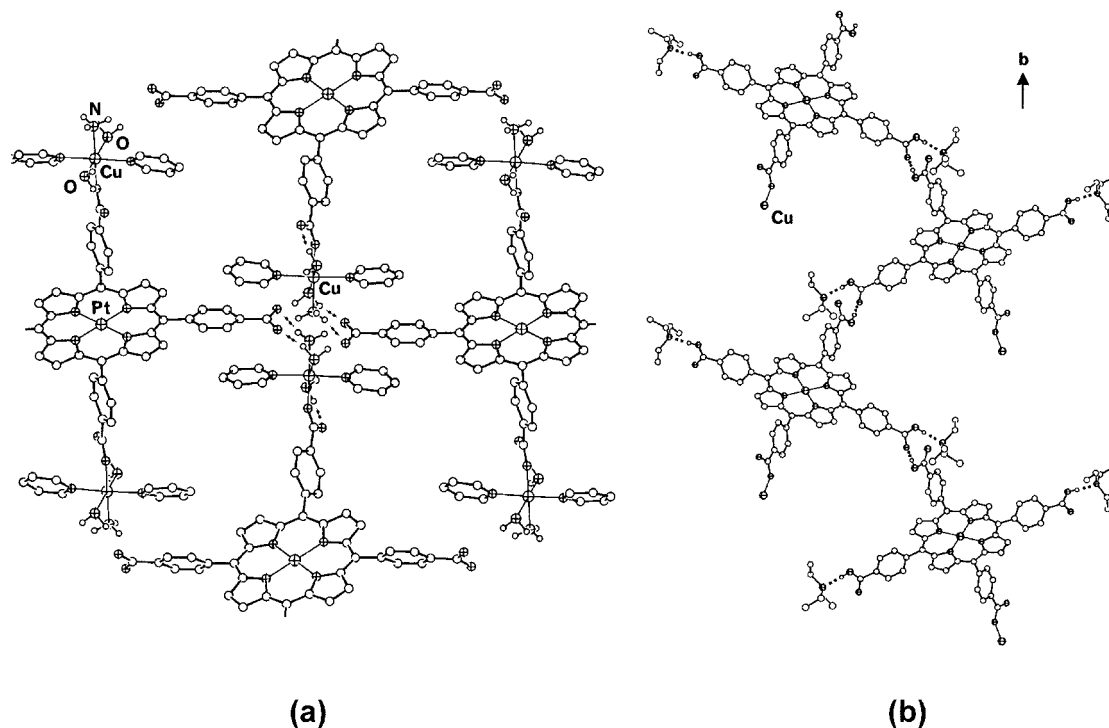**(a)**   **(b)**

Figure 4. Illustration of the hydrogen bonds: (a) between adjacent molecules in the *ac* plane in structure **1′**, and (b) porphyrin-porphyrin and porphyrin-triethylamine interactions in **2′**. All the protons attached to O and N are shown, and the H-bonds are denoted by dotted lines. In (a) the intramolecular H-bond is indicated as well, but the additional interactions present between molecules in different *ac* layers (Table 2) could not be shown.

phyrin sponges" described previously in the literature for the non-functionalized tetraphenylporphyrin (TPP) species [1, 2]. Thus, the two crystal structures consist of columnar arrangements of the porphyrin fameworks, which stack in an offset manner along the short *b* axis in **1′**, and along the *a* axis in **2′** (Figure 2). In order to allow for a condensed stacking, the planes of the porphyrin cores in both solids are inclined about 48° (in **1′**) and 60° (in **2′**) with respect to the column axis. Along the stacks, in **1′** the parallel offset between the centers of neighboring molecules is about 4.9 Å, and the intermolecular spacing is 3.83 Å. The considerable overlap of the porphyrin species and the relatively short interplanar distance are indicative of strong stacking interactions [15–17]. In **2′**, although not all the porphyrins appear to be ion-paired to the copper ions, an ordered stacked arrangement is maintained throughout the crystal. Here, the parallel offset between the centers of neighboring molecules is 6.9 Å, which places the carboxyphenyl arms of one unit above of the porphyrin core of next molecule, with minimal overlap between the core macrocycles. The mean interplanar distance between adjacent porphyrin macrocycles is 4.11 Å.

The "ackward" molecular shapes of the two copper-porphyrin complexes are not complementary in three dimensions as far as their crystal packing is concerned, giving rise to the formation of wide channels between the columnar motifs, a common characteristic of the porphyrin clathrates [1, 2]. In both structures (Figure 3) neighboring columns are related by the screw/glide symmetry, and are characterized by differently oriented molecules, yielding a herring-bone arrangements of the porphyrin columns. In **1′**, weak hydrogen bonds, which involve the peripheral copper-coordinated

H_2O and NH_3 proton donors and the carboxylate acceptors, occur between the columns (Table 2, Figure 4). Correspondingly, a cross-section parallel to the *ac* plane through the structure reveals an open supramolecular square-grid. Each grid point of this pattern represents a "meeting point" between the proton donor (copper end) and proton acceptor (carboxylate end) arms of four porphyrin units (Figures 3a and 4a). Regular stacking of such grids along *b* creates channel voids, which are occupied by the pyridine solvent. The hydrogen bonds link between molecules within the *ac* plane, as well as between adjacent molecular layers displaced along *b*.

The open organization of the porphyrin columns in **2′** reveals similar clathrate features accommodating in the channel voids molecules of the triethylamine base and an additional disordered water (Figure 3b). It is held together by a series of hydrogen bonds, involving all the potential proton donors in this structure (Table 2). First, the two molecules of triethylamine are involved as proton acceptors in interactions with two of the carboxylic groups. This is evidenced by rather short O· · ·N contacts of 2.64 and 2.67 Å, which connect the solvent molecules to the channel walls and minimize their possible disorder (as opposed to the disordered pyridine species in the former example). In addition, strong hydrogen bonds form between the porphyrin units of adjacent stacks related by the screw axis and aligned roughly along the *b* axis (the first and the third molecule in such hydrogen-bonded chain are related by one unit translation along *b*), as it is indicated by a corresponding distance OH7· · ·O5 of 2.54 Å (Table 2, Figure 4b). The water molecules lie also within a hydrogen-bonding distance from the surrounding
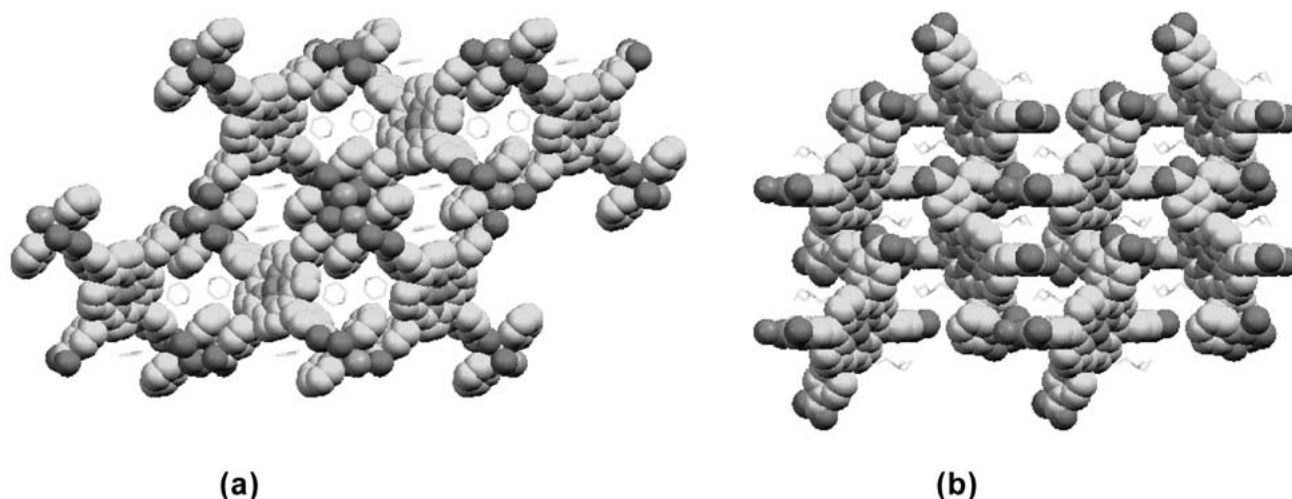
Figure 5. Space-filling illustration of the channel-type clathrates viewed down the channel axes (as in Figure 3). The guest components are indicated by line framework. (a) **1'** – structure viewed down *b*, (b) **2'** – structure viewed down *a* (the water molecules enclathrated within the channels are not shown).

carboxylic groups, providing additional links between the Pt-TCPP columns.

Conclusions

Our efforts to formulate porphyrin-based network materials of high structural rigidity which resemble molecular-sieve structures and zeolite analogues by utilizing diverse synthetic (in the crystal-engineering sense) strategies, occasionally lead to undesired products. This observation reflects also on the "odds and ends" of solid-state synthesis by solvothermal techniques which appears to be extremely sensitive to subtle variations in the experimental conditions and composition of the reaction mixture. Thus, in the present case, the solvothermal reaction of the Pt-TCPP building blocks with external copper ion templates yielded only discrete coordination complexes (**1** and **2**) between the two species instead of extended coordination polymers. This is explained by blockage of the coordination sites of the copper ions by other strong ligands as pyridine, water and NH_3. In several respects the crystal packing of the assembled solids **1'** and **2'** is similar to that observed in the large majority of common TPP clathrates. The expanded (by coordination with Cu) metalloporphyrin units form a corrugated pattern of offset-stacked porphyrin components at regular intervals of about 3.8–4.1 Å [17]. Such relatively short interporphyrin distance is feasible as the Pt-TCPP units lack axial binding capacity to the porphyrin center. The overall architectures of **1'** and **2'** are characterized by channels that propagate through the crystal, between the porphyrin columns, parallel to the stacking axis. The porphyrin stacks are linked to each other by a series of hydrogen bonds, involving effectively all the proton donors present in these componds [18]. The surfaces of the porphyrin core macrocycles line the channel walls, with ample space above and below them to accommodate the pyridine of triethylamine guest components. A space-filling illustration of the two clathrates is given in Figure 5, emphasizing the open nature of the porphyrin host lattices which formed. Network materials composed of the Pt-TCPP

tectons and copper-ion linkers have been described recently [19].

Supporting information available

The crystallographic data for **1'** and **2'** have been deposited with the Cambridge Structural Database in the CIF format (CCDC 211799 and CCDC 211800).

Acknowledgements

References

1. M.P. Byrn, C.J. Curtis, Y. Hsiou, S.I. Khan, P.A. Sawin, S.K. Tendick, A. Terzis, and C.E. Strouse: *J. Am. Chem. Soc.* **115**, 9480 (1993).
2. M.P. Byrn, C.J. Curtis, I. Goldberg, Y. Hsiou, S.I. Khan, P.A. Sawin, S.K. Tendick, and C.E. Strouse: *J. Am. Chem. Soc.* **113**, 6549 (1991).
3. P. Dastidar, Z. Stein, I. Goldberg, and C.E. Strouse: *Supramol. Chem.* **7**, 257 (1996).
4. Y. Diskin-Posner and I. Goldberg: *Chem. Commun.*, 1961–1962 (1999).
5. Y. Diskin-Posner, S. Dahal, and I. Goldberg: *Angew. Chem. Int. Ed.* **39**, 1288 (2000).
6. Y. Diskin-Posner, S. Dahal, and I. Goldberg: *Chem. Commun.*, 585 (2000).
7. Y. Diskin-Posner and I. Goldberg: *New J. Chem.* **25**, 899 (2001).
8. Y. Diskin-Posner, G.K. Patra, and I. Goldberg: *Eur. J. Inorg. Chem.*, 2515 (2001).
9. M.E. Kosal, J.-H. Chou, S.R. Wilson, and K.S. Suslick: *Nat. Mater.* **1**, 118 (2002).
10. I. Goldberg: *Chem. Eur. J.* **6**, 3863 (2000).
11. I. Goldberg: *Cryst. Eng. Comm.* **4**, 109 (2002).
12. A. Altomare, M.C. Burla, M. Camalli, M. Cascarano, C. Giacovazzo, A. Guagliardi, and G. Polidori (SIR-97): *J. Appl. Crystallogr.* **27**, 435 (1994).

13. G.M. Sheldrick (SHELXL-97): Program for the Refinement of Crystal Structures from Diffraction Data, University of Göttingen, Germany (1997).
14. See for example: F.A. Cotton and G. Wilkinson: in *Advanced of Inorganic Chemistry*, Wiley & Sons, New York (1980).
15. C.A. Hunter, M.N. Meah, and J.K.M. Sanders: *J. Am. Chem. Soc.* **112**, 5773 (1990).
16. C.A. Hunter and J.K.M. Sanders: *J. Am. Chem. Soc.* **112**, 5525 (1990).
17. K. Krishna Kumar, S. Balasubramanian, and I. Goldberg: *Inorg. Chem.* **37**, 541 (1998).
18. M.C. Etter: *J. Phys. Chem.* **95**, 4601 (1991).
19. M. Shmilovits, Y. Diskin-Posner, M. Vinodu, and I. Goldberg: *Cryst. Growth Des.* **3**, 855 (2003).